Negative Sustain Waveform for Improving Discharge Characteristics in AC Plasma Display Panel

Jae Kwang Lim and Heung-Sik Tae, *Senior Member, IEEE*

***Abstract*—The discharge characteristics produced by a negative sustain waveform were examined in comparison with those produced by a positive sustain waveform. An image-intensified charge-coupled device (ICCD) revealed that the negative sustain waveform produced a faster and stronger sustain discharge than the positive sustain waveform. Simulation results also showed that the fast and strong sustain discharge produced by the negative sustain waveform was induced due to the rapid acceleration of the negative wall charges, such as electrons, when applying the negative sustain waveform directly to the electrode with negative wall charges, such as electrons. As a result, the luminance and luminous efficiency were both improved by about 14% and 13%, respectively, with a negative sustain pulse of −180 V when compared to the results with a positive sustain waveform of 180 V.**

***Index Terms*—Fast and strong sustain discharge, image-intensified charge-coupled device (ICCD) observation, improvement of luminance and luminous efficiency, negative sustain waveform, 2-D fluid simulation.**

I. Introduction

THE LUMINANCE and luminous efficiency of current plasma display panels (PDPs) still need to be improved in order to realize a high-quality PDP, particularly a full high-definition PDP (full HD PDP). Thus, to improve the sustain discharge characteristics without modifying the current PDP structure, various sustain driving waveforms have been proposed and extensively studied [1]–[13]. However, all the sustain waveforms that have already been studied have a positive amplitude, whereas negative sustain waveforms have so far been neglected. Experimental results have shown that, unlike positive sustain waveforms, negative sustain waveforms can produce a fast discharge ignition and intensive vacuum ultraviolet (VUV), thereby improving the discharge characteristics of PDPs. Therefore, since a high Xe gas chemistry and large sustain gap have already been investigated to improve the luminous efficiency of current PDPs [14]–[22], negative sustain waveforms also need to be seriously considered [23].

Accordingly, this paper examined the discharge characteristics induced by a negative sustain waveform and then compared them with those induced by a conventional positive sustain waveform. The discharge characteristics for both sustain waveforms were monitored using an image-intensified charge-coupled device (ICCD) camera, and a comparison was made on the discharge currents, corresponding infrared (IR) emissions, consumption powers, luminance, and luminous efficiency. In particular, to investigate the factors inducing a different sustain discharge with the positive and negative sustain waveforms, the electron density profile, ion density profile, and wall charge distributions of both sustain waveforms were compared using a 2-D fluid-model-based simulation.

Manuscript received March 26, 2008; revised June 27, 2008. Current version published September 24, 2008. This work was supported by the BK21 Project. The review of this paper was arranged by Editor V. R. Rao.

The authors are with the School of Electrical Engineering and Computer Science, Kyungpook National University, Daegu 702-701, Korea (e-mail: hstae@ee.knu.ac.kr).

Color versions of one or more of the figures in this paper are available online at http://ieeexplore.ieee.org.

Digital Object Identifier 10.1109/TED.2008.2003227

II. Comparison of Discharge Characteristics for Positive and Negative Sustain Waveforms

A. Experimental Results: IR Emissions, Wall Charge Behavior, and ICCD Observations for Positive and Negative Sustain Waveforms

Fig. 1(a) shows the driving waveforms for measurement applied to the three electrodes in a 7-in test panel to investigate the discharge characteristics and related wall charge behavior of the positive and negative sustain waveforms. Sustain pulses with an amplitude of 180 V were alternately applied to the X and Y electrodes to produce the sustain discharge, resulting in the accumulation of wall charges on the three electrodes after the application of the final X sustain pulse. Following a sufficient time delay to allow the priming effect to be completely eliminated, detecting ramp-type pulses with a positive or negative polarity, as shown in Fig. 1(b), were applied. In this case, ramp-type pulses, instead of square-type pulses, were used as the detecting pulses to enable a more detailed investigation of the discharge phenomenon. The ramp-type pulse can determine the firing voltage more accurately than the square-type pulse because the discharge initiation is easily discernible due to a slow increase of the applied voltage. The use of the ramp-type pulse as the detecting pulse, in this case, is the same case as the use of the ramp-type pulse in the analysis of V_t closed curve [24]–[27].

Fig. 1(b) shows the four different ramp-type detecting pulses with the same slope and absolute amplitude value. The wall charge distributions prior to the application of the ramp-type detecting pulses were exactly the same in all cases. In cases 1 and 4, detecting pulses with an amplitude of 210 V were applied to the Y and X electrodes, respectively, whereas in cases 2 and 3, detecting pulses with an amplitude of −210 V were applied to the Y and X electrodes, respectively. Fig. 1(c) shows the corresponding IR emissions measured from the 7-in test panel when applying the four different detecting pulses after the final X sustain discharge. Since atoms emitting 823- and 828-nm Xe are precursors of $Xe^*(^3P_2)$ excited-state atoms

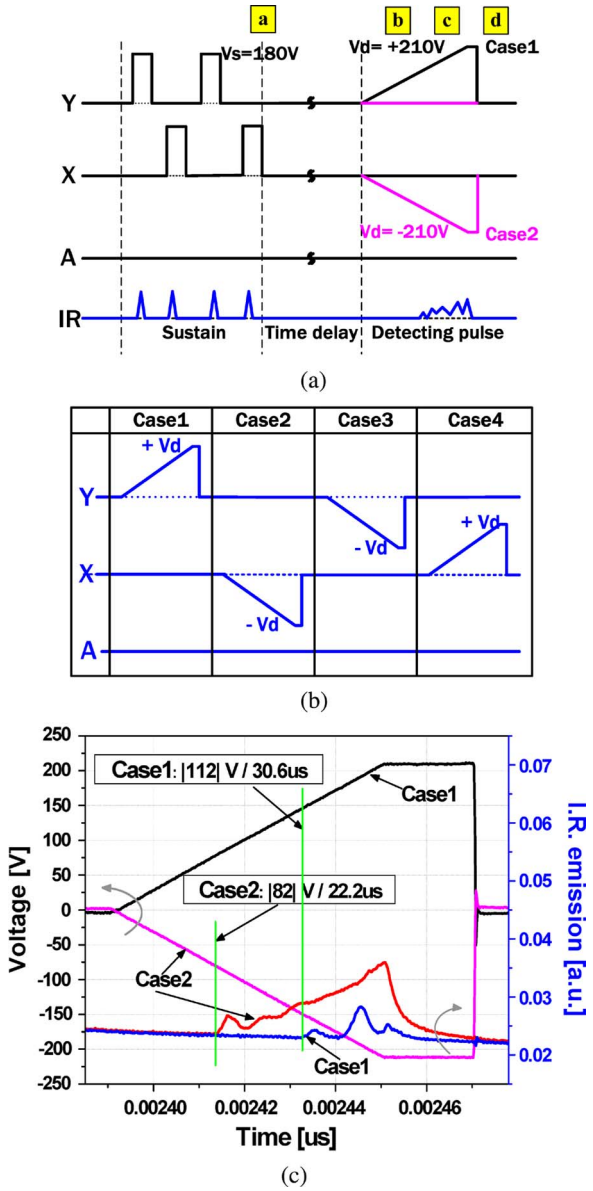

Fig. 1. (a) Measurement of driving waveforms applied to three electrodes in a 7-in test panel to investigate discharge characteristics and related wall charge behavior of positive and negative sustain waveforms. (b) Four different ramp-type detecting pulses with the same slope and absolute amplitude value. (c) IR emissions measured from a 7-in test panel when applying four different detecting pulses after the final X sustain discharge.

emitting 173-nm photons and of $Xe^*(^3P_1)$ excited-state atoms emitting 147-nm photons, respectively [28], IR is inevitably emitted prior to the VUV emission during the discharge. The IR emission is directly proportional to the intensity of the VUV [29], [30]. Therefore, in this experiment, the IR emissions were measured to monitor the changes in the luminous characteristics of the discharge relative to the various detecting pulses.

Since the final sustain discharge was produced by a positive pulse applied to the X electrode, no IR emission was detected in cases 3 and 4, whereas IR emission was observed in cases 1 and 2, as shown in Fig. 1(c). When comparing cases 1 and 2, the discharge was initiated faster at a low voltage ($|-82|$ V) in case 2 (= negative pulse). Furthermore, the discharge in

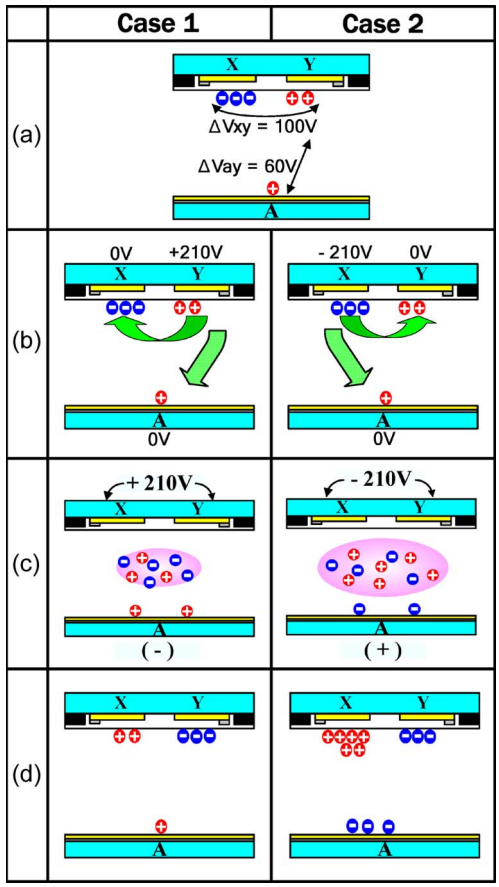

Fig. 2. Wall charge model for each step (a, b, c, and d) in Fig. 1(a), based on the experimental data in Fig. 1(c) for cases 1 and 2.

case 2 was maintained for a longer time than that in case 1 (= positive pulse). As a result, the total IR emission in case 2 was higher than that in case 1.

Fig. 2 shows a schematic model to describe the wall charge behavior at each step (a, b, c, and d) in Fig. 1(a), based on the experimental data obtained from Fig. 1(c). Prior to the application of the detecting pulse, i.e., after the final X sustain discharge produced by the positive sustain pulse, electrons were accumulated on the X electrode, whereas ions were accumulated on both the Y and A electrodes. In case 1, a positive detecting pulse was applied to the Y electrode with positive wall charges, such as ions, whereas in case 2, a negative detecting pulse was applied to the X electrode with negative wall charges, such as electrons. As shown in (c) and (d) in Fig. 2, in case 2, the application of a negative detecting pulse to the electrode with negative wall charges induced a stronger discharge, resulting in the accumulation of more wall charges on the three electrodes.

Fig. 3 shows the IR images taken by the ICCD camera during the discharges produced by the positive and negative sustain waveforms. As shown in Fig. 3, for the negative sustain waveform, the discharge was initiated after 430 ns, and the intensive discharge maintained for 15 ns longer, ranging from 445 to 460 ns. Meanwhile, with the positive sustain waveform, the major discharge started slowly after 445 ns, with the intensive discharge produced after 475 ns and maintained for a shorter time. Therefore, the ICCD illustrated that the

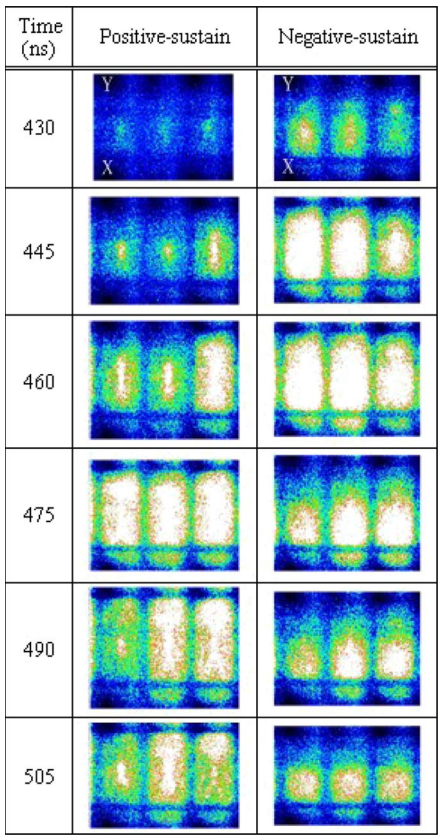

Fig. 3. IR images taken by the ICCD camera during discharges produced by positive and negative sustain waveforms.

negative sustain waveform produced a faster and stronger sustain discharge than the positive sustain waveform.

B. Simulation Results: Ion/Electron Density Profiles and Wall Charge Distribution for Positive and Negative Sustain Waveforms

A numerical analysis using a 2-D fluid model was applied [31], including Poisson, continuity, and drift–diffusion equations [32]. It was assumed that the local field approximation, i.e., the ionization and excitation rates, was a function of the local field [33]. The reaction model consisted of eight levels for Xe and six levels for Ne, and the secondary electron coefficient was assumed to be 0.2 for the Ne ions and 0.02 for the Xe ions [34].

Fig. 4 shows the simulation results for the electron and ion density profiles when square-type positive and negative sustain waveforms were applied to the sustain electrodes. As shown in Fig. 4, with the negative sustain waveform, particularly after 422 ns, the electrons moved more rapidly directly from the Y $(= -180$ V$)$ electrode toward the X $(= 0$ V$)$ electrode in the vicinity of the sustain electrodes. Conversely, with the positive sustain waveform, the electrons moved more slowly from the Y $(= 0$ V$)$ electrode toward the X $(= +180$ V$)$ electrode via the phosphor layer. For the ion density profile, as shown in Fig. 4, larger amounts of ions moved toward the phosphor layer when applying the positive sustain waveform, meaning that a positive sustain waveform can potentially cause severe damage to the phosphor layer.

Therefore, the simulation results confirmed that the discharge produced by the negative sustain waveform, unlike the positive sustain waveform, had distinctive features. First, direct application of the negative sustain waveform to the sustain electrode accumulating electrons caused a rapid acceleration of the electrons, thereby inducing a fast and intense discharge within the cell. Second, the application of the negative sustain waveform caused electrons to accumulate on the phosphor layer, thereby reducing the damage to the phosphor layer based on minimizing the heavy ions impinging on the address electrode during a strong sustain discharge.

Fig. 5 shows the simulation results for the wall charges accumulating on the three electrodes after a sustain discharge produced by square-type positive and negative sustain waveforms. With the positive sustain waveform, electrons were accumulated on the X electrode, whereas ions were accumulated on both the Y and A electrodes. Meanwhile, with the negative sustain waveform, electrons were accumulated on both the X and A electrodes, whereas ions were accumulated on the Y electrode. However, the total amount of wall charges accumulated on the three electrodes was almost the same for both sustain waveforms, unlike the experimental results in Fig. 1(c).

III. Luminous Characterisitcs With Positive and Negative Sustain Waveforms

Fig. 6(a) and (b) shows the driving waveforms employed in this paper, including the reset, address, and sustain periods, where (a) is the positive and (b) is the negative sustain waveform during a sustain period. A 7-in ac PDP filled with a Ne–Xe (4%) gas mixture at 400 torr was used as the test panel. The test panel had a conventional ac PDP structure with stripe barrier ribs and three electrodes, namely, two sustain electrodes and one address electrode. The voltage levels ranged from 150 to 200 V for the positive sustain pulse and from -150 to -200 V for the negative sustain pulse under a sustain frequency of 100 kHz. The detailed specifications for the 7-in test panel are listed in Table I.

Fig. 7 shows a schematic diagram of the optical and electrical measurement system used to measure the luminous efficiency of the test panel with the two different sustain waveforms. The measurement system consisted of the 7-in test panel, its driving circuit system, an ampere meter, and a color analyzer. The driving circuit system consisted of a pair of positive sustain driving circuits (A) and negative sustain driving circuits (B), plus two power supplies, namely, P1 and P2. The driving circuit was used to supply the electrical pulses to the X and Y sustain electrodes and A address electrode. The real currents that flowed through the three electrodes during a sustain discharge were then measured as follows. The sustain currents flowing through the X and Y sustain electrodes during a sustain period were measured in the power line between the driving circuit and the power supply using a digital ampere meter. The additional switch loss during a sustain period was also included in the power consumption, as the currents were measured in front of the driving circuits, as shown in Fig. 7. The luminance of the visible lights emitted from the 7-in test panel was measured

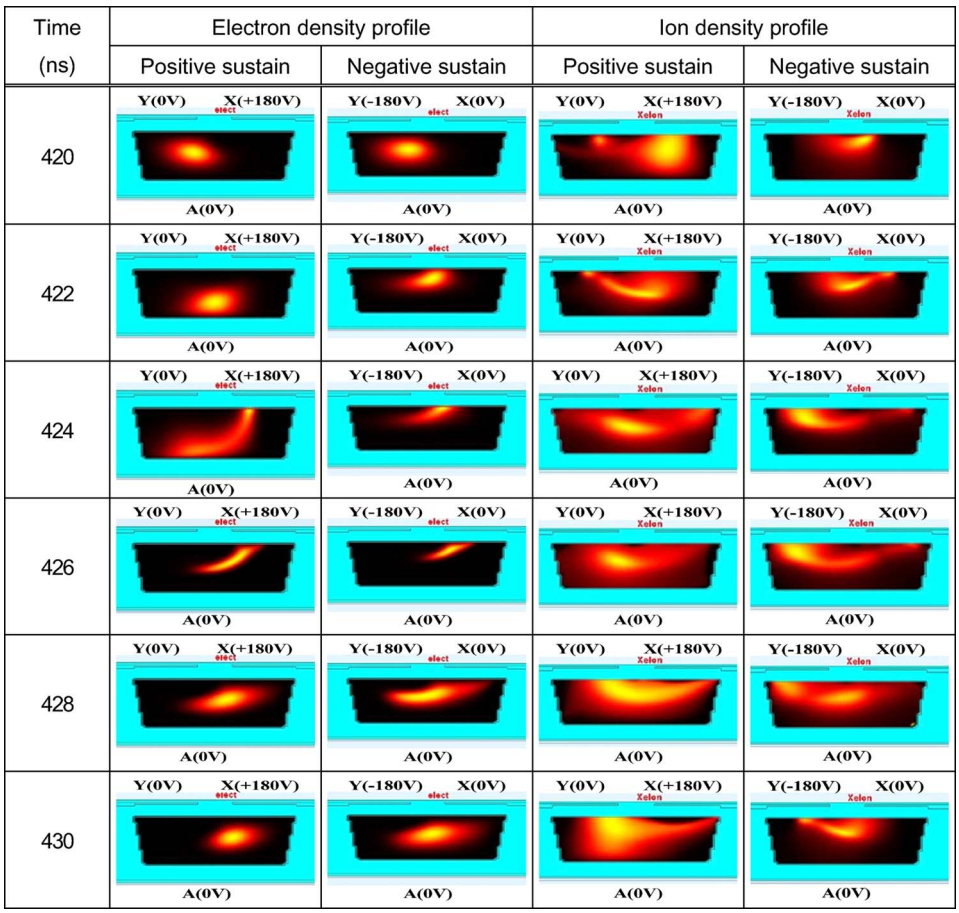

Fig. 4. Simulation results for electron and ion density profiles when applying positive and negative sustain waveforms to sustain electrodes.

using a color analyzer (CA-100), and the luminous efficiency was obtained from the following [35]:

$$\text{Luminous efficiency}\left(\frac{lm}{W}\right) = \frac{\pi \times \text{Luminance}\left(\frac{\text{cd}}{\text{m}^2}\right) \times \text{Display area}\,(\text{m}^2)}{\text{Power consumption}\,(\text{W})}. \quad (1)$$

The power consumption in (1) is the sum of the powers consumed through the X, Y, and A electrodes. The power consumption through the X and Y electrodes was calculated from both the applied voltage using the power supply and the discharge current passing through the ampere meter.

Fig. 8(a) and (b) shows the negative and positive voltages and related IR emissions measured when the 100 sustain pulses were applied at 100 kHz. Fig. 8(c)–(e) shows the enlarged displacement and discharge currents and the IR emission waveforms when applying the positive and negative sustain waveforms, respectively.

In Fig. 8(c), the voltage amplitude was 180 V for the positive sustain waveform and -180 V for the negative sustain waveform. In Fig. 8(c), the positive and negative sustain waveforms exhibited the same rising and falling voltage slopes, respectively, and the corresponding displacement and discharge currents in Fig. 8(d) were measured under the same voltage slope conditions. As shown in Fig. 8(e), when applying the negative sustain waveform, the initiation point of IR emission was shifted to the left, and the IR emission peak was also higher, implying that the sustain discharge was produced faster and stronger in the case of applying the proposed negative sustain waveform, which was also confirmed by the discharge current in Fig. 8(d). However, the discharge current with the negative sustain waveform was slightly increased, as shown in Fig. 8(d).

Fig. 9(a) shows the corresponding luminance and power consumption when applying the positive and negative sustain pulses. The luminance of the negative sustain waveform was much higher than that of the positive sustain pulse, whereas the power consumption of the negative sustain waveform was only slightly increased. The resultant luminous efficiency data are shown in Fig. 9(b). In particular, with a negative sustain voltage of -180 V, the luminance was improved by about 14%, resulting in a luminous efficiency improvement of about 13% when compared to that with the positive sustain waveform. The improvement in the luminous efficiency under the negative sustain conditions was mainly due to the increased luminance rather than the reduced power consumption. As shown in Fig. 8(e), a high IR emission was obtained under the negative sustain conditions, implying that the increased IR emission resulted in an increase in the visible emission, as the IR emission was directly proportional to the intensity of the VUV. The simulation results also showed that direct application of the negative sustain waveform to the sustain

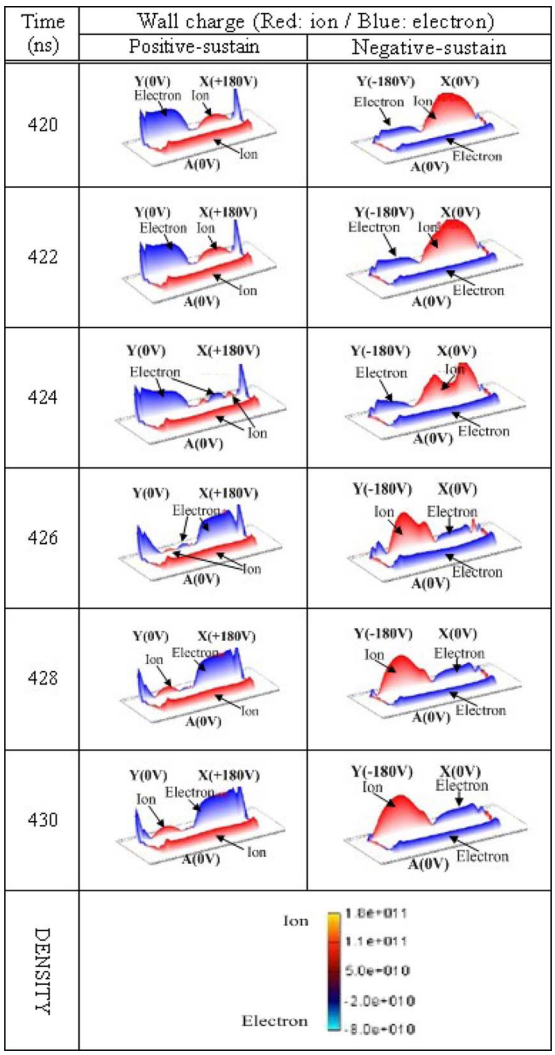

Fig. 5. Simulation results for the wall charges accumulated on the three electrodes after a sustain discharge produced by positive and negative sustain waveforms.

electrode accumulating electrons caused a rapid acceleration of the electrons, thereby inducing a fast and intense discharge within the cell. Our experimental observation was that the application of the negative potential to the negatively charged electrode could cause a fast increase in the amount of the electrons, thus resulting in an increase in the IR emissions. This phenomenon might be deeply related to the electron emission characteristics of the charged MgO surface, depending on the bias condition. That is, the emission characteristics of the charged MgO surface would depend strongly on the bias condition; the negative bias applied to the negatively charged MgO surface could facilitate the electron emissions from the MgO surface. This phenomenon should be further studied.

Table II shows the static margins (= firing voltage − minimum sustain voltage) measured and simulated for both types of sustain pulse. Here, a firing voltage means a voltage when all cells are in turn-on states, whereas a minimum sustain voltage means a voltage when all cells are changed completely from turn-on into turn-off states. In Table II, the experimental results were in good agreement with the simulation results, even though each voltage level had a slightly

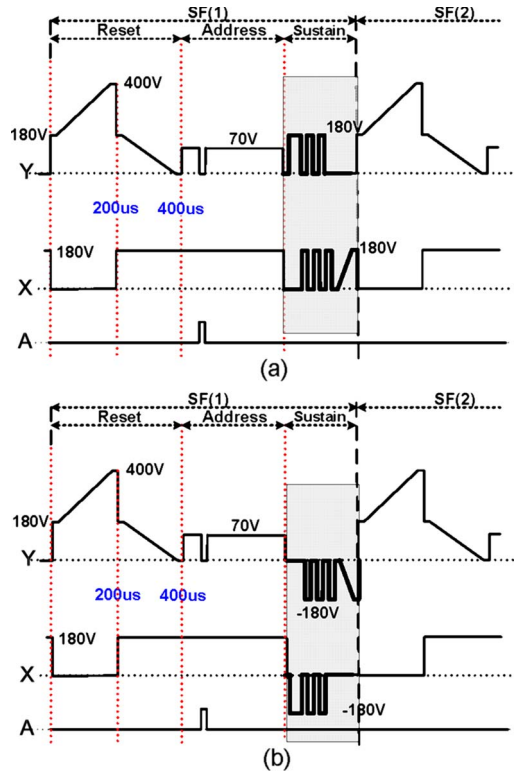

Fig. 6. Driving waveforms employed in this paper, including reset, address, and sustain periods, where (a) is the positive and (b) is the negative sustain waveform during a sustain period.

TABLE I
SPECIFICATIONS OF THE 7-in TEST PANEL EMPLOYED IN THIS PAPER

Front Panel		Rear Panel	
ITO width	310 μm	Barrier rib width	80 μm
ITO gap	60 μm	Barrier rib height	125 μm
Bus width	100 μm	Address width	100 μm
Bus lines		42	
Cell pitch		360	
Pressure		400 Torr	
Gas chemistry		Ne-Xe (4 %)	
Barrier-type rib		Stripe-type rib	

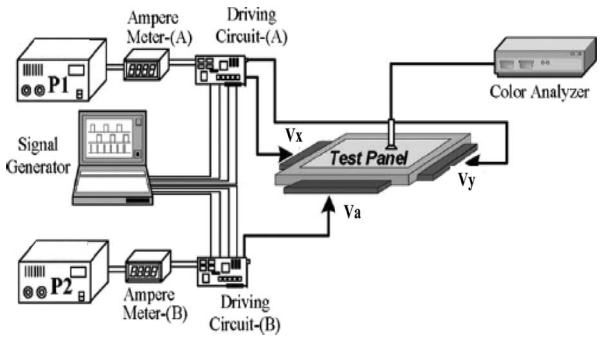

Fig. 7. Schematic diagram of the optical and electrical measurement system used to measure luminous efficiency.

different value. As shown in Table II, the static margin did not change, irrespective of the sustain pulse type, whereas the firing voltage and minimum sustain voltage were about 7–8 V lower with the negative sustain waveform. This decrease in the firing voltage and minimum sustain voltage was related to the fast initiation of the discharge when applying the negative

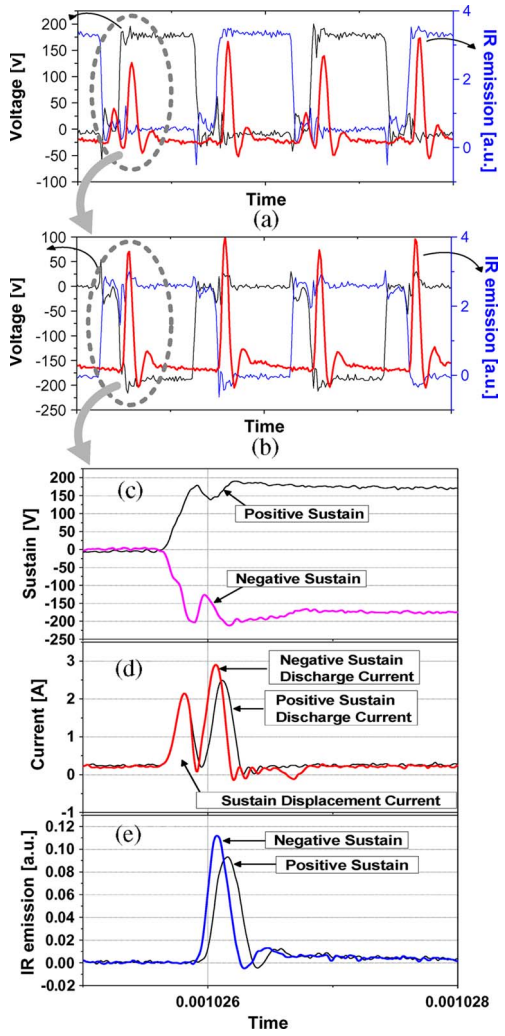

Fig. 8. (a) Positive sustain pulse of 180 V and negative sustain pulse of −180 V, plus (b) the associated displacement and discharge currents, and corresponding IR emissions.

sustain waveform. The fast initiation phenomenon was apparently mainly due to the rapid acceleration of the electrons induced when applying the negative sustain pulse to the electrode accumulating the electrons, as shown in the simulation in Fig. 4(a).

IV. Conclusion

The effects of positive and negative sustain waveforms on the sustain discharge characteristics were examined and compared in a 7-in test panel with a Ne–Xe (4%) gas mixture at 100 kHz. An ICCD revealed that the negative sustain waveform was able to produce a faster and stronger sustain discharge than the positive sustain waveform. Simulation results also showed that the fast and strong sustain discharge induced by the negative sustain waveform was mainly due to the rapid acceleration of the electrons when applying the negative sustain waveform directly to the sustain electrode with negative wall charges, such as electrons. As a result, the luminance and luminous efficiency were both improved by about 14% and 13%, respectively, with a negative sustain voltage of −180 V. Thus, it is expected that a negative sustain waveform can play a significant role in improving the discharge characteristics, particularly in the case of very small size cells, such as full-HD-PDP cells.

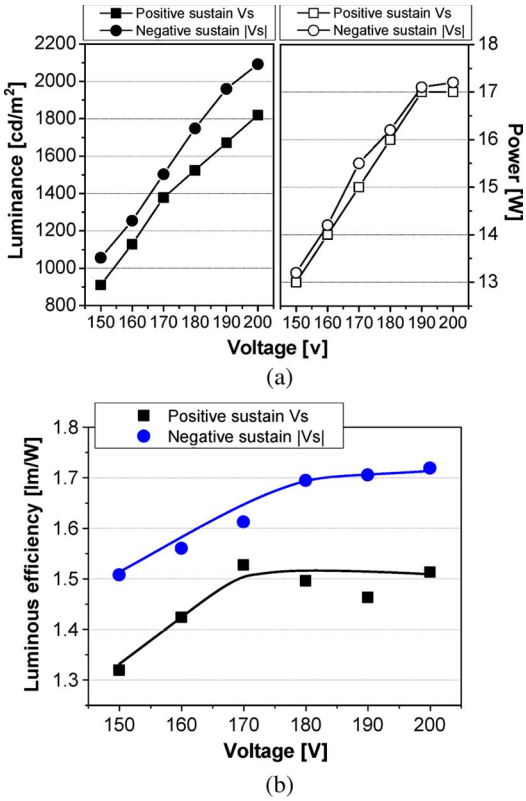

Fig. 9. (a) Luminance and power consumption and (b) luminous efficiency related to positive and negative sustain waveforms.

TABLE II
Static Margins for Positive and Negative Sustain Pulses

	Experiment		Simulation	
	Positive Sustain	Negative Sustain	Positive Sustain	Negative Sustain
V_f	205 V	198 V	230	200
V_{sm}	145 V	137 V	170	140
ΔV	60 V	61 V	60	60

References

[1] S.-H. Jang, K.-D. Cho, H.-S. Tae, K. C. Choi, and S.-H. Lee, "Improvement of luminance and luminous efficiency using address voltage pulse during sustain-period of AC-PDP," *IEEE Trans. Electron Devices*, vol. 48, no. 9, pp. 1903–1910, Sep. 2001.

[2] H.-S. Tae, K. D. Cho, S.-H. Jang, and K. C. Choi, "Improvement in the luminous efficiency using ramped-square sustain waveform in an AC surface-discharge plasma display panel," *IEEE Trans. Electron Devices*, vol. 48, no. 7, pp. 1469–1472, Jul. 2001.

[3] T. Hashimoto and A. Iwata, "Improvement of luminous efficiency in an AC-PDP by self-erasing discharge waveform," in *Proc. SID Dig.*, 1999, pp. 540–543.

[4] S. T. Lo and C. L. Chen, "Improving luminous efficiency of AC-type plasma display panels by adjusting the state of sustaining discharges in the sustaining period," *IEEE Trans. Plasma Sci.*, vol. 30, no. 1, pp. 428–435, Feb. 2002.

[5] J. K. Kim, J. H. Yang, J. H. Seo, and K. W. Whang, "The improvement of discharge characteristics by the use of asymmetric pulse driving in an alternating current plasma display panel," *IEEE Trans. Plasma Sci.*, vol. 29, no. 2, pp. 377–382, Apr. 2001.

[6] S. T. Lo and C. H. Chen, "A new mixed-mode sustain method to improve the luminous efficiency of alternating current plasma display panels," *IEEE Trans. Electron Devices*, vol. 49, no. 5, pp. 762–769, May 2002.

[7] G. Veronis and U. S. Inan, "Improvement of the efficiency of plasma display panels by combining waveform and cell geometry design," *IEEE Trans. Plasma Sci.*, vol. 33, no. 1, pp. 147–156, Feb. 2005.
[8] H.-S. Tae, B.-G. Cho, and S.-I. Chien, "Self-erasing discharge mode for improvement of luminous efficiency in AC plasma display panel," *IEEE Trans. Electron Devices*, vol. 50, no. 2, pp. 522–524, Feb. 2003.
[9] J. C. Ahn, Y. Shintani, K. Tachibana, T. Sakai, and N. Kosugi, "Effects of pulsed potential on address electrode in a surface-discharge alternating-current plasma display panel," *Appl. Phys. Lett.*, vol. 82, no. 22, pp. 3844–3846, Jun. 2003.
[10] J. Kang, O. D. Kim, W. G. Jeon, J. W. Song, J. Park, J. R. Lim, and J. P. Boeup, "Panel performance of RF PDP," in *Proc. IDW Dig.*, 2000, pp. 643–646.
[11] J. Kang, "High luminance and luminous efficiency in PDPs driven by radio-frequency pulses," *J. SID.*, vol. 8, pp. 223–226, 2000.
[12] Y. M. Li, C. L. Chen, and H. B. Hsu, "Improve the luminous efficiency of AC plasma display by high-frequency driving on address electrodes," *IEEE Trans. Electron Devices*, vol. 50, no. 4, pp. 913–917, Apr. 2003.
[13] H.-S. Tae, H. J. Seo, D.-C. Jeong, J. H. Seo, H. Kim, and K.-W. Whang, "Analysis of microdischarge characteristics induced by synchronized auxiliary address pulse based on cross-sectional infrared observation in AC plasma display panel," *IEEE Trans. Plasma Sci.*, vol. 33, no. 2, pp. 931–940, Apr. 2005.
[14] L. F. Weber, *Positive Column AC Display*, Feb. 6, 2001.
[15] T. Callegari, J. Ouyang, N. Lebarq, B. Caillier, and J.-P. Boeuf, "3D modeling of a plasma display panel cell," in *Proc. Eurodisplay*, 2002, pp. 735–738.
[16] K. C. Choi, N. H. Shin, K. S. Lee, B. J. Shin, and S.-E. Lee, "Study of various coplanar gaps discharges in ac plasma display panel," *IEEE Trans. Plasma Sci.*, vol. 34, no. 2, pp. 385–389, Apr. 2006.
[17] H. Kim and H.-S. Tae, "Firing and sustaining discharge characteristics in alternating current microdischarge cell with three electrodes," *IEEE Trans. Plasma Sci.*, vol. 32, no. 3, pp. 488–492, Jun. 2004.
[18] J. Y. Kim, H. Kim, H.-S. Tae, J. H. Seo, and S.-H. Lee, "Effect of voltage distribution among three electrodes on microdischarge characteristics in AC-PDP with long discharge path," *IEEE Trans. Plasma Sci.*, vol. 34, no. 6, pp. 2579–2587, Dec. 2006.
[19] J. Ouyang, T. Callegari, J. P. Caillier, and B. Boeuf, "Large-gap AC coplanar plasma display cells: Macro-cell experiments and 3-D simulations," *IEEE Trans. Plasma Sci.*, vol. 31, no. 3, pp. 422–428, Jun. 2003.
[20] G. Oversluizen, T. Dekker, M. F. Gillies, and S. T. de Zwart, "High-Xe-content high-efficacy PDPs," *J. SID.*, vol. 12, no. 1, pp. 51–55, 2004.
[21] D. Hayashi, G. Heusler, G. Hagelaar, and G. Kroesen, "Discharge efficiency in high-Xe-content plasma display panels," *J. Appl. Phys.*, vol. 95, no. 4, pp. 1656–1661, Feb. 2004.
[22] W. J. Chung, B. J. Shin, T. J. Kim, H. S. Bae, J. H. Seo, and K.-W. Whang, "Mechanism of high luminous efficient discharges with high pressure and high Xe-content in AC PDP," *IEEE Trans. Plasma Sci.*, vol. 31, no. 5, pp. 1038–1043, Oct. 2003.
[23] J. K. Lim, C.-S. Park, B.-T. Choi, H.-S. Tae, S.-I. Chien, J. P. Park, N. S. Jung, and K.-S. Lee, "Improvement of luminance and luminous efficiency using new negative sustain waveform in AC-plasma display panel," in *Proc. SID Dig.*, 2006, pp. 597–600.
[24] H.-S. Tae, S.-K. Jang, K.-D. Cho, and K.-H. Park, "High-speed driving method using bipolar scan waveform in AC plasma display panel," *IEEE Trans. Electron Devices*, vol. 53, no. 2, pp. 196–204, Feb. 2006.
[25] K. Sakita, K. Takayama, K. Awamoto, and Y. Hashimoto, "High-speed address driving waveform analysis using wall voltage transfer function for three terminals and V_t close curve in three-electrode surface-discharge AC-PDPs," in *Proc. SID*, 2001, pp. 1022–1025.
[26] H. J. Kim, J. H. Jeong, K. D. Kang, J. H. Seo, I. H. Son, K. W. Whang, and C. B. Park, "Voltage domain analysis and wall voltage measurement for surface-discharge type ac-PDP," in *Proc. SID*, 2001, pp. 1026–1029.
[27] H. Inoue, Y. Seo, K. Sakita, and Y. Hashimoto, "Numerical analysis of V_t close curve for non-uniform wall charge distribution in three-electrode AC-PDP," in *Proc. Eurodisplay*, 2002, pp. 931–934.
[28] N. Uemura, Y. Yajima, Y. Kawanami, K. Suzuki, N. Kouchi, and Y. Hatano, "Kinetic model of the VUV production in AC-PDPs as studied by time-resolved emission spectroscopy," in *Proc. IDW Dig.*, 2000, pp. 639–642.
[29] W. G. M. Shao, J. R. Gottschalk, M. Brown, and A. D. Compaan, "Vacuum ultraviolet emission dynamics of a coplanar electrode microdischarge: Dependence on voltage and Xe concentration," *J. Appl. Phys.*, vol. 92, no. 2, pp. 682–689, Jul. 2002.
[30] G. Oversluizen, M. Klein, S. de Zwart, S. van Heusden, and T. Dekker, "Improvement of the discharge efficiency in plasma displays," *J. Appl. Phys.*, vol. 91, no. 4, pp. 2403–2408, Feb. 2002.
[31] J. H. Seo, W. J. Chung, C. K. Yoon, J. K. Kim, and K. W. Whang, "Two-dimensional modeling of a surface type alternating current plasma display panel cell: Discharge dynamics and address voltage effects," *IEEE Trans. Plasma Sci.*, vol. 29, no. 5, pp. 824–831, Oct. 2001.
[32] H. C. Kim, M. S. Hur, S. S. Yang, S. W. Shin, and J. K. Lee, "Three-dimensional fluid simulation of a plasma display panel cell," *J. Appl. Phys.*, vol. 91, no. 12, pp. 9513–9520, Jun. 2002.
[33] J. Meunier, P. Belenguer, and J. B. Boeuf, "Numerical model of an AC plasma display panel cell in neon–xenon mixture," *J. Appl. Phys.*, vol. 78, no. 2, pp. 731–745, Jul. 1995.
[34] J. Y. Kim, H. Kim, H.-S. Tae, J. H. Seo, and S.-H. Lee, "Effect of voltage distribution among three electrodes on microdischarge characteristics in AC-PDP with long discharge path," *IEEE Trans. Plasma Sci.*, vol. 34, no. 6, pp. 2579–2587, Dec. 2006.
[35] C.-H. Park, S.-H. Lee, D.-H. Kim, Y.-K. Kim, and J.-H. Shin, "A study on the new type sustaining electrode showing high luminous efficiency in AC PDPs," *IEEE Trans. Electron Devices*, vol. 48, no. 10, pp. 2255–2259, Oct. 2001.

Jae Kwang Lim received the M.S. degree in electronic and electrical engineering from Kyungpook National University, Daegu, Korea, in 2006, where he is currently working toward the Ph.D. degree in electronic engineering.

He is currently with the School of Electrical Engineering and Computer Science, Kyungpook National University. His current research interests include plasma physics, driving waveform, driver circuits of plasma display panels, and display integrated circuits.

Heung-Sik Tae (M'00–SM'05) received the B.S., M.S., and Ph.D. degrees in electrical engineering from Seoul National University, Seoul, Korea, in 1986, 1988, and 1994, respectively.

Since 1995, he has been a Professor with the School of Electrical Engineering and Computer Science, Kyungpook National University, Daegu, Korea. His research interests include the optical characterization and driving waveform of plasma display panels.

Dr. Tae is a member of the Society for Information Displays. He has been an Editor for the IEEE TRANSACTIONS ON ELECTRON DEVICES section on flat panel displays since 2005.